The Dispersants Effect on Physical Properties of Long-Lasting Luminescent Polypropylene

Shin-Cheng Jang,[1] Yao-Chi Shu,[2] Fu-Sheng Chuang,[3] Wen-Chin Tsen,[3] Jing-Dong Chow,[4] Chien-Chung Chen[5]

[1]*Department of Fashion Design, Ling Tung University, Taichung, Taiwan, Republic of China*
[2]*Department of Applied Cosmetology, Lee-Ming Institute of Technology, Taipei, Taiwan, Republic of China*
[3]*Department of Materials Science and Engineering, Vanung University, Tao-Yuan, Taiwan, Republic of China*
[4]*Department of Environmental Engineering, Vanung University, Tao-Yuan, Taiwan, Republic of China*
[5]*Department of Oral Medicine, Taipei Medical University, Taipei, Taiwan, Republic of China*

Received 17 June 2010; accepted 23 July 2011
DOI 10.1002/app.35442
Published online 6 December 2011 in Wiley Online Library (wileyonlinelibrary.com).

ABSTRACT: Two series of blends, O-PP_{15} and O-PP_{35}, were prepared by mixing polypropylene (PP), luminescent powders ($SrAl_2O_4$: Eu^{2+}, Dy^{3+}) of 15 and 35 μm average particle diameter, and hydrophobic dispersant at about 190°C in the Brabender mixer. The effect of amounts and diameter of luminescent powders on the physical properties of PP material were discussed herein. The luminescence and afterglow time tests indicated that the initial luminescence of all blends increased with the luminescent powders amounts. O-PP_{35} blends showed lower afterglow luminance than O-PP_{15} blends at low luminescent powder amounts. The melting and crystallization temperatures of the blends appeared at 152–168°C and 87–103°C, respectively. The blends displayed peaks attributable to a α crystal structure at $2\theta = 18°–19°$. The β crystal structure was only evident from its characteristic 2θ peak at 15°–16° in the WAXD pattern of the O-PP_{35} blends with high luminescent powder amounts. All of the blends had lower tensile strengths. However, the improvement in the luminescent powder distribution was evident from the SEM images after adding hydrophobic dispersant. © 2011 Wiley Periodicals, Inc. J Appl Polym Sci 124: 4645–4654, 2012

Key words: polypropylene; dispersant; luminescence; afterglow

INTRODUCTION

Luminescent materials have been widely applied in many areas recently. Materials of this kind absorb ultraviolet light from natural or indoor light sources, and store this energy for subsequent light emission in the dark. The stored energy is gradually converted into visible light, such that the luminescence could last from a few hours up to 10 hours.[1–3] Because of this illuminating property, such materials are widely used in the areas of fire safety, architecture decoration, and transportation, and they have been incorporated into plastics, rubbers, and fibers.[4]

The materials studied in the present research belong to a rare-earth aluminate class of luminescent materials, with compositions of $SrAl_2O_4$: Eu^{2+}, Dy^{3+}. Acting as the luminescent center, the divalent europium ion (Eu^{2+}) absorbs ultraviolet- and visible-light of wavelengths below 480 nm. In the land of electronic rail, the electron transits from $4f^65d^1$ to $4f^7$, resulting in a characteristic yellowish-green light of wavelength 520 nm. The incorporation of Dy^{3+} results in the establishment of an appropriate energy level at room temperature, which prolongs the luminescence time. Such light-emitting materials not only display wide luminescence and excitation spectra, but also high quantum efficiencies, long afterglow times, and excellent stability and performance, and they are also nonradioactive. By virtue of these advantages, materials of this class are used in many areas.[5–9]

The light-emitting mechanism of luminescent materials has been an extensive research area. Since the discovery of a long-lasting luminescence phenomenon upon doping of $SrAl_2O_4$ powder with Dy^{3+} and Eu^{2+}, many researchers have directed their efforts towards understanding the mechanism.[10–12] Furthermore, some of these researchers have utilized knowledge gained from luminescence research to understand the mechanism of long-lasting light-emitting glass. One of these mechanisms is that of hole-transfer.[13–17] Through the hole-transfer mechanism, it is widely recognized that Eu^{2+} is transformed to Eu^{1+}, and that Dy^{3+} is transformed to Dy^{4+} through capturing unoccupied holes during the activation process ($Dy^{3+} + hole^+ \rightarrow Dy^{4+}$). However, the existence of these unusual valence charges

Correspondence to: W.-C. Tsen (charity@mail.vnu.edu.tw).

on europium and dysprosium (Eu^{1+} and Dy^{4+}) has not been proven experimentally in light-emitting materials after excitation. Through an experiment in which luminescent glass was exposed to X-ray and laser irradiation, Qiu and Hirao[18] demonstrated that doping does not change the charge of an ion; hence, the credibility of the hole-transfer model has been questioned. In addition, Qiu and Hirao[18] proposed a bit-based coordinate model to illustrate the mechanism of light-emitting glass. Holes are created when Re^{3+} ions replace the divalent rare-earth ions. Eu^{2+}-activated luminescent glasses are generally prepared under vacuum conditions, and this result in oxygen vacancies. The defect levels are generally the energy level of holes or oxygen vacancies. Under the influence of an external light source, electrons are promoted from the ground to the excited state. Some of these electrons fall back to the light-emitting low-energy level. The rest of the electrons are stored in the defect levels through relaxation. When the electrons in the defect levels absorb energy, the restimulation returns them to the excited state. These electrons then fall back to the ground-state energy level, and as a result the material is illuminated. The duration of the luminescence is related to the number of electrons stored in the defect levels and the amount of energy absorbed through heat. The greater the number of electrons in the defect level, the longer the afterglow time. The more energy absorbed, the easier it is for the electrons to overcome the energy gap between the defect level and the excited state. Light emitted through radiation coupling, specifically through excitation by an external light source, is regarded as light-induced fluorescence or photo stimulated luminescence.

Because of its low hygroscopicity, durability, good chemical stability, and resistance to micro-organisms, polypropylene (PP) has become one of the most widely used materials. Recently, the fierce competition of newly developed materials has driven down the price of PP. The low price of PP with respect to good quality product and moldability has resulted in renewed interest in this material. To develop the applications of PP, in the present work strontium aluminate-based luminescent materials have been melted and blended with PP under specific conditions. The luminescent materials (powder) used in this study had a specific gravity of 3.6; hence, direct addition of the luminescent powder to molten PP would have resulted in deposition. In addition, PP is hydrophobic and the luminescent powder is an organic salt; hence, these two materials do not distribute uniformly due to their unfavorable interaction. To solve this mixing problem of luminescent powder and PP, hydrophobic polyethylene oxide-based dispersants were added.

TABLE I
Mixing Ratios of the Samples

Code	Amount of luminescent powder (phr)
O-PP_{15}-1	1
O-PP_{15}-2	2
O-PP_{15}-3	3
O-PP_{15}-4	4
O-PP_{15}-5	5
O-PP_{15}-10	10
O-PP_{35}-1	1
O-PP_{35}-2	2
O-PP_{35}-3	3
O-PP_{35}-4	4
O-PP_{35}-5	5
O-PP_{35}-10	10

phr, parts per hundreds of resin.

O-PP_{15}-X and O-PP_{35}-X: PP samples with hydrophobic dispersant, luminescent powder of 15 μm and 35 μm diameter and X phr luminescent powder, respectively.

Amount of hydrophobic dispersant: 1 phr.

EXPERIMENTAL

Materials

PP powder (Ha Chin). Rare earth strontium aluminate luminescent powder (Ta Li): thermal resistance of 500°C, afterglow time of 12 h, luminescence color of yellow green (YG), average particle diameters of 15 and 35 μm. Dispersants (En Hou): hydrophobic polyethylene oxide-based dispersants.

Preparation of the samples

Mixtures of PP and luminescent powder (luminescent PP) were prepared at different ratios. The amount of hydrophobic dispersant was fixed at 1 phr. The materials were mixed at 190°C in a Brabender mixer. The ratios of the mixtures are listed in Table I.

Measurements

1. Melt index (MI): the weight (g) of PP material flowing through a 2.1 mm pore at 44 psi and 170–190°C in 10 min.
2. Spectrophotometry: Emissions were measured using a fluorescence spectrophotometer (SPF-500C, SLM.AMINCO). A 300 W pressurized xenon lamp was used as the excitation light source, with dual-monochromator scanning. The phosphorescence spectra (i.e., afterglow spectra) of the materials were recorded with a Shimadzu UV-2100 spectrophotometer.
3. Luminescence and afterglow time: These were measured using a GB1048-1779 apparatus. The measurement was commenced 6 min after exposure to light of wavelength 254 nm.

4. Differential scanning calorimetry (DSC): Thermal analysis of the samples was performed on a Perkin-Elmer Pyris 1 DSC instrument. Experiments were carried out with a liquid nitrogen cooler in a helium atmosphere. The mass of each sample was ~ 5–8 mg. Heating measurements on the specimens were carried out from −100 to 220°C at a rate of 20°C/min. Thereafter, the samples were cooled from 220°C to −100°C at a rate of 100°C/min. A second heating measurement was then performed from −100 to 220°C at a rate of 20°C/min.
5. Wide-angle X-ray diffraction (X-ray): The sample was placed in an oven at 220°C for 5 min to erase its thermal history. Testing conditions: (a) 30 kV, (b) 10 mA, with angle from 60°–65°, (c) chart speed 10 mm/min, (d) diffraction speed of 4° radiation/min, (e) camera distance 3.5 cm, (f) exposure time 3 h, and (g) Ni-filtered Cu-K_α radiation.
6. Scanning electron microscopy (SEM): The characteristics of the surface and cross-section were observed by SEM.
7. Mechanical tensile strength analyzer (MTS): The tensile strength of the material was tested. Testing conditions: specimen size 5 × 1 cm^2, thickness 0.3–0.5 mm, chuck speed 20 mm/min, and maximum load 10 kg

RESULTS AND DISCUSSION

Melt index

The melt indexes (MI) of the samples are listed in Table II. The MI of pure PP powder is 24.1 g/10 min. The MI of O-PP_{15}-X and O-PP_{35}-X samples (abbreviated O-PP_{15} and O-PP_{35}) are 30.1–36.5 g/10 min and 28.9–35.6 g/10 min, respectively, presenting the high MI of samples with dispersant and luminescent powder. The MI of the 35 μm luminescent powder sample was slightly lower than that of the 15 μm sample. Higher friction results from the rigidity of the luminescent powder; hence, the MI is lowered as the amount of luminescent powder diameter is increased.

TABLE II
Melt Indexes (MI) of the Samples

Code	MI (g/10 min)
O-PP_{15}-1	36.5
O-PP_{15}-2	35.7
O-PP_{15}-3	34.1
O-PP_{15}-4	33.5
O-PP_{15}-5	32.8
O-PP_{15}-10	30.1
O-PP_{35}-1	35.6
O-PP_{35}-2	33.7
O-PP_{35}-3	32.8
O-PP_{35}-4	31.6
O-PP_{35}-5	30.5
O-PP_{35}-10	28.9
PP_{15}-1	23.7
PP_{15}-3	22.8
PP_{15}-5	21.5
PP_{15}-10	20.4

The MI of pure PP: 24.1 g/10 min.

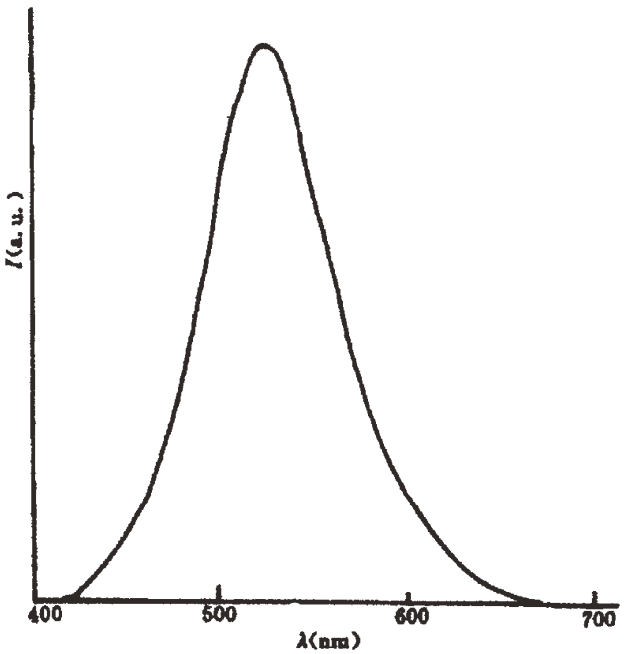

Figure 1 The luminescence spectrum of the luminescent powder (λ_{max} = 520 nm).

The luminescent PP without dispersant (PP_{15}: PP with luminescent powder diameter of 15 μm) were prepared to understand the effect of dispersant on PP. The MI of PP_{15}-1, PP_{15}-3, PP_{15}-5, and PP_{15}-10 samples are 23.7, 22.8, 21.5, and 20.4 g/10 min, respectively. Comparing the MI of O-PP_{15} and PP_{15}, the addition of the dispersant enhances the flowability of the samples. Since, the luminescent powder used in this study was in ionic form, the interaction between the luminescent powder and the dispersant was favorable. The luminescent powder was dispersed uniformly throughout the sample (interaction decreases the contact surface area of luminescent powder with PP, thereby reducing friction and improving flowability).

Spectrophotometry

The luminescence spectrum of the luminescent powder used in this study is shown in Figure 1. The maximum luminous intensity is located at 520 nm (λ_{max}), the wavelength of yellow–green light. The optical absorption spectrum of the luminescent powder is shown in Figure 2. A maximum is seen in the ultraviolet region, a characteristic emission band of Eu^{2+} and Dy^{3+}. This explains why ultraviolet and

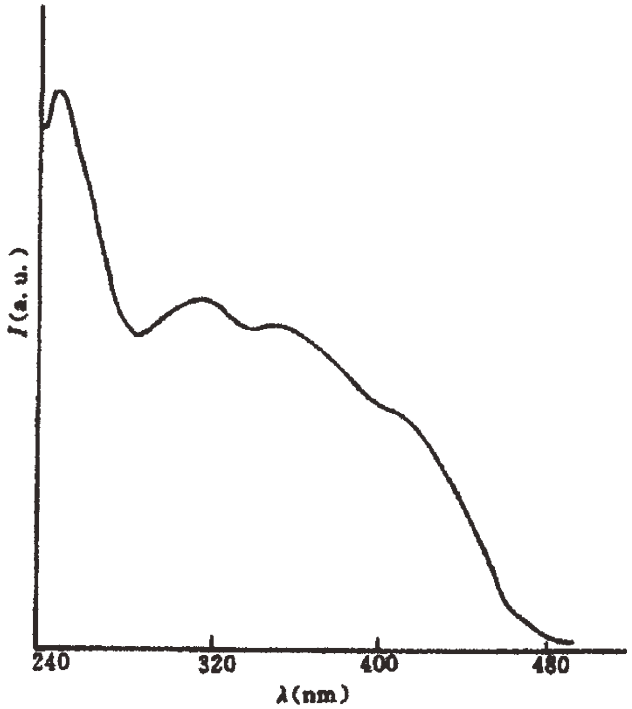

Figure 2 The optical absorption spectrum of the luminescent powder ($\lambda_{max} = 254$ nm).

blue light are effective in stimulating the luminescence of the luminescent powder. The luminous intensity reaches a maximum at 254 nm (λ_{max}). Therefore, UV light of 254 nm was chosen for all luminance tests to ensure consistency.[19,20]

Luminescence and afterglow time

New materials can be created through mixing of long-lasting and light-emitting powder with other materials such as metal sheets, fiber fabric, etc. To achieve the best luminance characteristics, transparent plastic with good UV light penetration is preferable. The UV light is required for luminescent powder excitation. The substrate used in this study, PP, would undergo chain breaking if it were exposed to daylight. Therefore, a UV-absorbing agent is usually added to PP during the manufacturing process to prevent its chain breaking. However, the addition of such a UV-absorbing agent to PP also reduces the absorption characteristics of the luminescent powder, thereby affecting the afterglow.

The initial luminescence of the pure luminescent powder was 1151 mcd/m^2. Table III shows the initial luminances of the samples in the range 39–439 mcd/m^2. The PP translucency, dispersant, diameter of luminescent powder, and amounts of luminescent powder and UV-absorbing agent plays significant roles in affecting the initial luminescence. The initial luminescences of PP_{15} samples (contain 15 μm luminescent powder) increase from

TABLE III
The Initial Luminances of the Samples

Code	Initial luminescence (mcd/m^2)
O-PP_{15}-3	66
O-PP_{15}-5	126
O-PP_{15}-10	246
O-PP_{35}-3	39
O-PP_{35}-5	87
O-PP_{35}-10	439
PP_{15}-3	42
PP_{15}-5	50
PP_{15}-10	187

42 to 187 mcd/m^2 as the amount of luminescent powder increases. An improvement in the initial luminescence is seen upon the addition of hydrophobic dispersant. The O-PP_{15} samples (contain 15 μm luminescent powder and hydrophobic dispersant) have initial luminescences in the range 66–246 mcd/m^2, higher than those of the samples without dispersant. The MI results show the improvement in the flowability of O-PP_{15} samples. This improvement may be attributed to the dispersing effect. Therefore, the dispersing agent improves both the initial luminescence and the flowability. Comparing to O-PP_{15} samples, the initial luminescences of O-PP_{35} samples in the range 39–439 mcd/m^2 show low initial luminescences in low amount luminescent powder and high initial luminescences in high amount luminescent powder.

Figures 3–5 show that the luminescent powder (rare earth aluminate) used in this study has a typical luminescence decay curve.[21] The luminous intensity decays rapidly during the initial stage (0–120 s). Subsequently, the luminescence of the samples was measured at intervals of 120 s, which showed a slowing down of the luminescence decay.

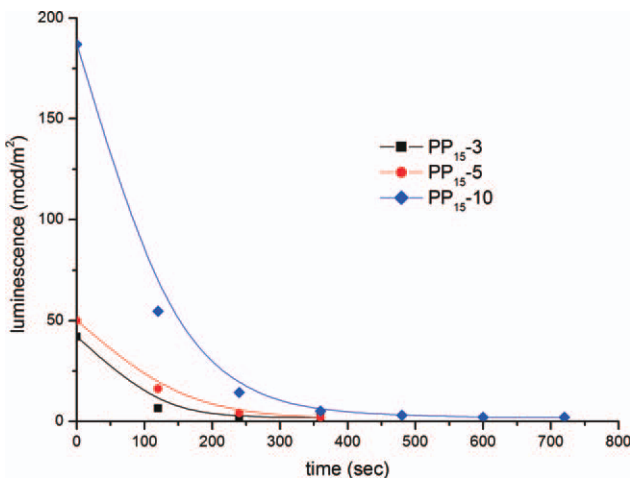

Figure 3 Luminescence decay curves of the PP_{15}-3, PP_{15}-5, and PP_{15}-10 samples. [Color figure can be viewed in the online issue, which is available at wileyonlinelibrary.com].

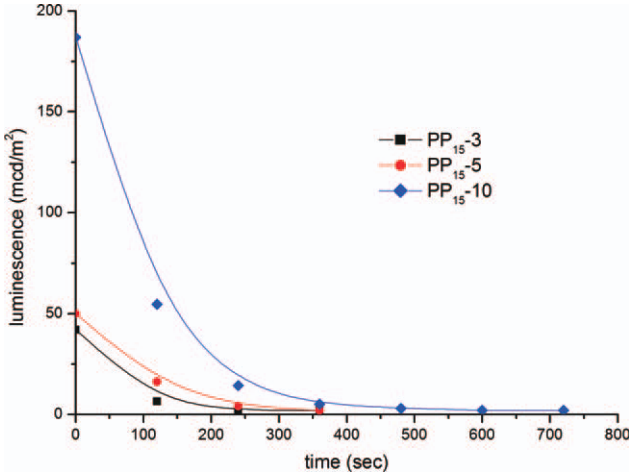

Figure 4 Luminescence decay curves of the O-PP_{15}-3, O-PP_{15}-5, and O-PP_{15}-10 samples. [Color figure can be viewed in the online issue, which is available at wileyonlinelibrary.com].

The luminescence curves of samples containing different amounts of 15 μm luminescent powder (PP_{15}) are shown in Figure 3. The afterglow time increases with increasing amount of luminescent powder incorporated. The samples containing 3, 5, and 10 phr luminescent powder had afterglow times of 240, 320, and 550 s (to reach minimum luminance), respectively. PP_{15}-3 and PP_{15}-5 have very similar decay curves to PP_{15}-10. However, significant luminescence enhancement is seen in the decay curve for PP_{15}-10.

The luminescence decay curves of O-PP_{15} samples are shown in Figure 4. Among all of the luminescence decay curves in Figures 3 and 4, those of PP_{15}-3 and O-PP_{15}-3 show the greatest difference in the initial stage. After the initial stage, the decay curves overlap as time progresses. However, the samples containing 5 and 10 phr luminescent powders do not follow the same trend. The initial stage and the subsequent luminescence for the dispersant-containing samples are significantly higher.

The luminescence decay curves of O-PP_{35} are shown in Figure 5. The decay curve follows the same trend as that of the samples containing 15 μm luminescent powder shown in Figure 3; a larger amount of luminescent powder results in higher luminescence intensity.

In general, luminescence intensity is enhanced by larger diameter of the luminescent powder. However, the luminescence of samples containing less luminescent powder is not consistent with this general observation. From Table III, it can be seen that the sample containing 10 phr luminescent powders (PP_{35}-10) displayed the highest luminescence of 439 mcd/m^2. However, the initial luminescence of the O-PP_{35}-5 sample was higher than those of the PP_{15}-5 samples, but lower than that of the O-PP_{15}-5 sample. The initial luminescence of the O-PP_{35}-3 sample was lower than that of the PP_{15}-3 sample. A possible explanation for this phenomenon lies in the luminescent powder manufacturing process. Table II shows the MI of samples, indicating O-PP_{15} samples have higher flowability than O-PP_{35} samples. The flowability of samples depends on luminescent powder diameter, and then, the low flowability results from shear and friction forces between the luminescent powders or the luminescent powders and PP. The luminescent powder with larger diameter is more susceptible to shear and friction forces, and hence size reduction and color coating in the processing. The luminescence decay curves of the O-PP_{15}-10 and O-PP_{35}-10 samples are compared in Figure 6,

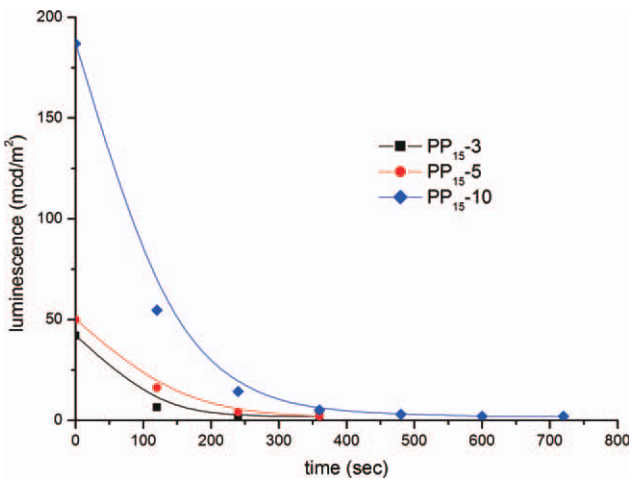

Figure 5 Luminescence decay curves of the O-PP_{35}-3, O-PP_{35}-5, and O-PP_{35}-10 samples. [Color figure can be viewed in the online issue, which is available at wileyonlinelibrary.com].

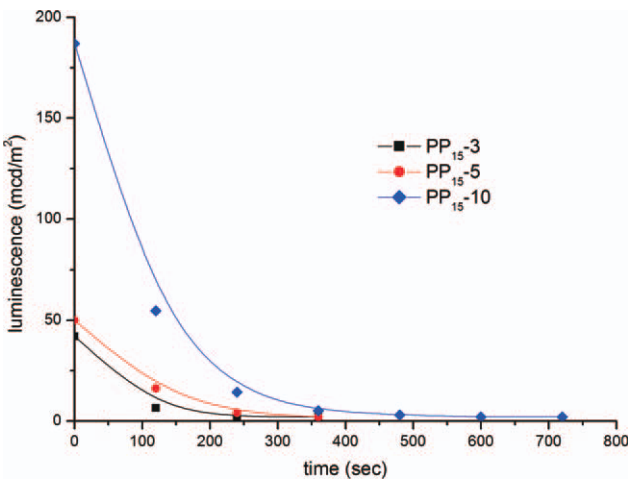

Figure 6 Luminescence decay curves of the O-PP_{15}-10 and O-PP_{35}-10 samples. [Color figure can be viewed in the online issue, which is available at wileyonlinelibrary.com].

showing the luminescence intensity enhancement and longer afterglow time for the sample with larger luminescent powder diameter.

Crystallization behavior

The mechanical properties of a polymer are determined by its crystal structure. Any alteration in crystallization will affect the mechanical properties directly. DSC and WAXD analyses have been used as important tools to study the modification of crystallization behavior.

To erase the thermal histories of the materials, samples were heated to 220°C. DSC cooling curves of the samples were obtained by cooling to −100°C at a rate of 100°C/min. Figure 7 shows the DSC cooling curves (70–120°C) of pure PP and O-PP_{15} samples. DSC heating curves were obtained by heating from −100 to 220°C at a rate of 20°C/min. The DSC heating curves in the temperature range from 130 to 180°C are shown in Figure 8. In Figure 7, the exothermic crystallization peak in the region from 85 to 110°C reaches a maximum at 99°C (T_c). In Figure 8, the crystalline melting peak appears in the region from 150 to 170°C and reaches a minimum at 166°C. The enthalpy (ΔH) associated with this peak is 77 J/g. The degree of crystallization (X_c) can be calculated from the enthalpy according to the following equation:

$$X_c = \Delta H/\Delta H^\circ \times 100\%$$

where ΔH° is the specific enthalpy of PP at 100% crystallization ($\Delta H^\circ = 209$ J/g). Therefore, the degree of crystallization (X_c) for pure PP is 36.8%.

The configuration of the PP molecular chain is a 3_1 spiral. Among the three most commonly observed

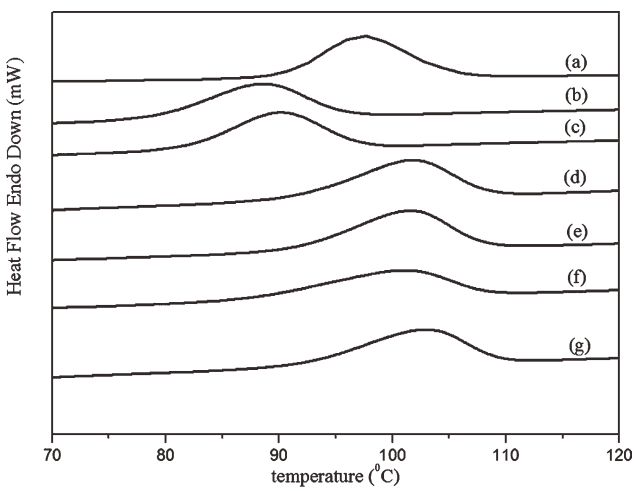

Figure 7 DSC cooling curves of pure PP and O-PP_{15} samples (a) pure PP, (b) O-PP_{15}-1, (c) O-PP_{15}-2, (d) O-PP_{15}-3, (e) O-PP_{15}-4, (f) O-PP_{15}-5 and (g) O-PP_{15}-10.

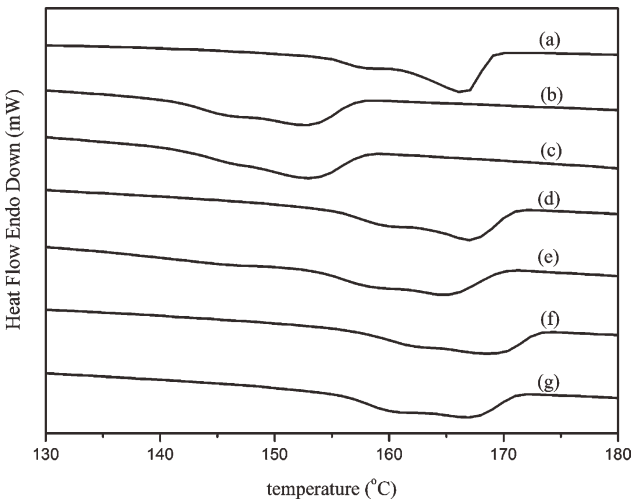

Figure 8 DCS heating curves at 130–180°C of pure PP and O-PP_{15} samples after melt-quenching (a) pure PP, (b) O-PP_{15}-1, (c) O-PP_{15}-2, (d) O-PP_{15}-3, (e) O-PP_{15}-4, (f) O-PP_{15}-5, and (g) O-PP_{15}-10.

different crystal structures, the monoclinic crystal (also called α crystalline) is the most stable structure. The characteristic 2θ peak of the α crystalline form is seen in WAXD in the range 18°–19°.[22–25] The lamellar crystalline structure is special. At the beginning of crystal formation, the crystal grows on the lamellar surface horizontally, eventually forming a reticular structure. The addition of a nucleating agent to the PP sample promotes the formation of the hexagonal β crystal form. The characteristic 2θ peak of the β crystal form is seen in WAXD in the region 15°–16°. The crystalline arrangement of the β crystal is looser than that of the α crystal. The β crystal structure has better impact resistance. The β crystal is converted into the α crystal upon heating. In early research, the third type of crystal structure was reported to be triclinic. However, recent research has revealed the crystal structure to be orthorhombic, also called the γ crystal. The characteristic 2θ peak of the γ crystal is seen in WAXD in the region from 19.2° to 20.5°. The γ crystal is formed when high-molecular-weight PP is subjected to high pressure or low molecular weight PP is under atmospheric pressure.

Figure 8 shows that a shoulder (in the vicinity of 158°C) appears prior to the melting peak of pure PP at 166°C. To ascertain whether the shoulder on the heating curve was a result of the formation of a different crystal form, a WAXD measurement was run on a PP sample. In Figure 9(a), the characteristic 2θ peak of the α crystal (18°–19°) is observed. However, the characteristic 2θ peaks of the β (15°–16°) and γ (19.2°–20.5°) crystals are not seen. Therefore, the PP crystalline structure consisted only of the α crystal. The appearance of a shoulder on the heating curve is due to the deformation of the α crystal.

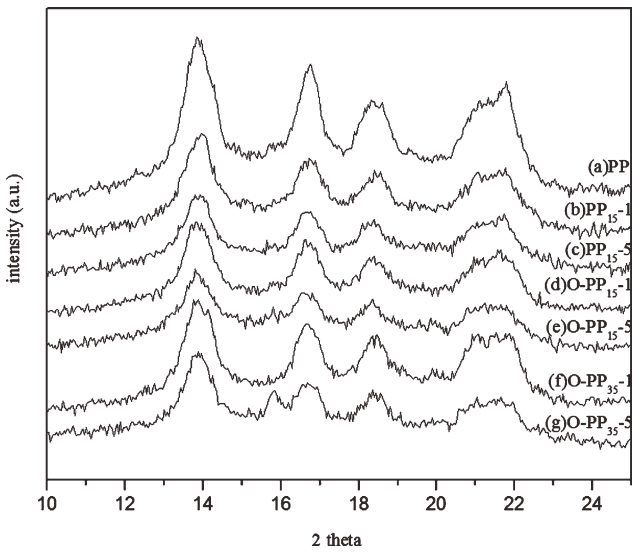

Figure 9 WAXD intensity patterns of the samples.

The two transition temperatures arise because of the difference in lamellar structures. The α crystal is in reticular form. The lower transition temperature of the shoulder is due to the melting of transverse lamellae. The higher transition temperature is due to the melting of radial lamellae (thicker crystal structure).

The heating and cooling DSC curves of the O-PP_{15} samples are shown in Figures 7 and 8, respectively. The heating DSC curve of O-PP_{15} features a shoulder and a melting peak. From Figures 7 and 8, the exothermic crystallization peak and crystalline melting peak of O-PP_{15}-1 and 2 samples are seen to be 75–100°C and 140–160°C, respectively. The DSC curves for the O-PP_{15}-1 and 2 samples are shifted to lower temperature ranges compared to that for pure PP. The exothermic crystallization peak and crystalline melting peak of O-PP_{15}-3, 4, 5, 10 samples are 85–115°C and 155175°C, respectively. The melting and crystallization temperatures of all samples are listed in Table IV. The Comparing O-PP_{15} samples with the pure PP sample, the T_c and T_m of the O-PP_{15}-1 and O-PP_{15}-2 samples are 10–15°C lower. This significant difference implies the formation of a new crystal structure. In Figure 9(d), the characteristic 2θ peak of α crystal is observed. However, this peak is lowered and broadened. The lowering of the peak signifies defective or incomplete crystallization. The broadened peak is a result of a wider distribution of α crystal sizes. Therefore, the defective α crystal may account for the lowered crystallization and melting temperatures.

The crystallization degree of the O-PP_{15}-1 sample is significantly lowered. According to the discussion in the previous section regarding the effect of the addition of minimal amounts of luminescent powder (1–2 phr) and hydrophobic dispersant to PP, the PP is first plasticized by the hydrophobic dispersant, and then the luminescent powder disrupts the polymer chains. The introduction of luminescent powder disrupts the crystallization of PP, which results in a defective crystal structure. The T_c and T_m ranges for the O-PP_{15}-3, 4, 5, and 10 samples are 101–103°C and 165–168°C, respectively. These ranges are very close to the T_m and T_c of pure PP. In Figure 9(e), the characteristic peak of the α-crystal is seen for the sample O-PP_{15}-5, indicating that no other crystal structures are present. However, the degree of crystallization of the O-PP_{15}-5 sample is lowered (Table IV). The excess luminescent powder may also account for the lowering of the degree of crystallization. Since, the sample was a mixture of PP,

TABLE IV
Thermodynamic Properties and Crystallization Degrees of the Samples

Code	Crystallization temperature T_c (°C)	Melting temperature T_m (°C)	Crystallization degree X_c (%)
O-PP_{15}-1	89	152	33.9
O-PP_{15}-2	90	153	33.5
O-PP_{15}-3	102	167	32.7
O-PP_{15}-4	101	165	32.1
O-PP_{15}-5	101	168	31.9
O-PP_{15}-10	103	167	30.0
O-PP_{35}-1	89	152	35.7
O-PP_{35}-2	89	152	35.5
O-PP_{35}-3	89	153	35.3
O-PP_{35}-4	87	152	34.8
O-PP_{35}-5	88	155	34.8
O-PP_{35}-10	88	153	34.0
PP_{15}-1	103	166	33.5
PP_{15}-3	89	152	32.8
PP_{15}-5	90	153	32.2
PP_{15}-10	91	154	31.5

For pure PP: $T_c = 99$°C, $T_m = 166$°C, $X_c = 36.8\%$.

hydrophobic dispersant, and luminescent powder, the components could react together in certain proportions. A small proportion of 1 phr hydrophobic dispersant contributes to the plasticization of PP, disrupting its crystallization. A larger proportion of dispersant interacts with the luminescent powder and the luminescent domain forms. In Table IV, the degrees of crystallization (X_c) of the O-PP_{15} samples are seen to be in the range 33.9–30.0%, showing a reduction in X_c as the amount of luminescent powder is increased. This X_c of O-PP_{15} is significantly lower than the X_c of pure PP (36.8%), signifying the effect of the hydrophobic dispersant and luminescent powder. From Figures 8 (d–g), the melting temperature from the DSC curve increases as the amount of luminescent powder is increased. Potentially, the increment of crystal thickness of α crystal could contribute to these temperature changes.

The characteristic crystal temperatures of the PP_{15} samples are listed in Table IV. They follow the same trend as seen for the samples containing dispersant; X_c decreases as the amount of luminescent powder is increased. The addition of small amounts of luminescent powder (PP_{15}-1, 2) did not result in different characteristic crystal temperatures (T_c and T_m) compared with the pure PP sample. However, when the luminescent powder amount was equal to or higher than 3 phr, the characteristic crystal temperatures decreased dramatically. WAXD patterns of the PP_{15}-1 and PP_{15}-5 samples showed the characteristic 2θ peak of the α crystal [Figs. 9(b,c)]. Through comparison of the results for the PP_{15}-1 and PP_{15}-5 samples with the WAXD pattern of pure PP, the crystal structures of PP_{15}-1 and 5 are evidently similar to that of pure PP. Therefore, without the addition of a dispersant, the α crystal structure of PP is not affected by small amounts of luminescent powder.

The effects of hydrophobic dispersant on the characteristic crystal temperatures and crystallization degree of samples containing 35 μm diameter luminescent powder (O-PP_{35}) were investigated. In Table IV, it can be seen that the crystallization and melting temperatures (T_c and T_m) of all of the O-PP_{35} samples were lower than those for pure PP. The amount of luminescent powder in these samples ranged from 1 to 10 phr. The degree of crystallization of O-PP_{35} ranged from 35.7 to 34.0%. The range of the crystallization degree in the O-PP_{35} sample is the highest among all of the samples. This phenomenon can be explained in terms of exclusion of the luminescent powder (35 μm) from the PP polymer chain due to its large particle size. Without the interference of the luminescent powder, the crystal structure is much more consistent, hence the higher X_c.

The WAXD patterns of O-PP_{35}-1 and O-PP_{35}-5 are shown in Figure 9(f,g). The characteristic peak of the α crystal is observed in both figures. Additionally, the characteristic peak of the β crystal also appears in the WAXD pattern of O-PP_{35}-5. In the previous discussion about the formation of the β crystal, it was mentioned that the β crystal is formed when a nucleating agent is incorporated into PP. It is likely, that a minor amount of the β crystal is formed in the O-PP_{35}-1 sample, but remains undetectable in the WAXD pattern as its peaks are lost in the noise.

Morphological observation

SEM images of PP_{15}-10, O-PP_{15}-10, and O-PP_{35}-10 are shown in Figure 10. Agglomeration of the luminescent particles is observed in Figure 10(a), but not in Figure 10 (b,c). The luminescent particles in Figure 10 (b,c) are distributed uniformly. These findings confirm the function of the dispersant in dispersing the luminescent particles. The SEM images in Figures 10 (b,c) show good adhesion at the interface between the luminescent particles and the substrate. The luminescent particles are distributed uniformly throughout the substrate. In spite of the addition of luminescent powder, the surface gloss is maintained in the new material.

Tensile strength

Pure PP has tensile strength and elongation at breaking of 41 MPa and 23%. Table V lists the tensile strengths and elongation at breaking of PP_{15} at around 25–30 MPa and 5–10%, respectively. The tensile strength and elongation decreases as the amount of luminescent powder is increased. Since, the luminescent powder is an inorganic salt, it does not interact favorably with PP, and so the sample is less capable of sustaining stress. In addition, the agglomeration of luminescent powder also contributes to the reduction in tensile strength and elongation.

The tensile strengths and elongation at breaking of the O-PP_{15} samples were 31–38 MPa and 11–19%, respectively. Similar to what was found for the PP_{15} samples, the tensile strength and elongation at breaking of the O-PP_{15} samples decreased as the amount of luminescent powder was increased. Comparing the tensile strength and elongation at breaking of PP_{15} with those of O-PP_{15} samples, the tensile strengths and elongation of O-PP_{15} are higher. The addition of hydrophobic dispersant improves the tensile strengths and elongation of the samples. When the hydrophobic dispersant plasticizes the PP, the polymer chains become loosely packed and hence much more randomized.

The tensile strengths and elongation at breaking of the O-PP_{35} samples were 30–36 MPa and 9–17%.

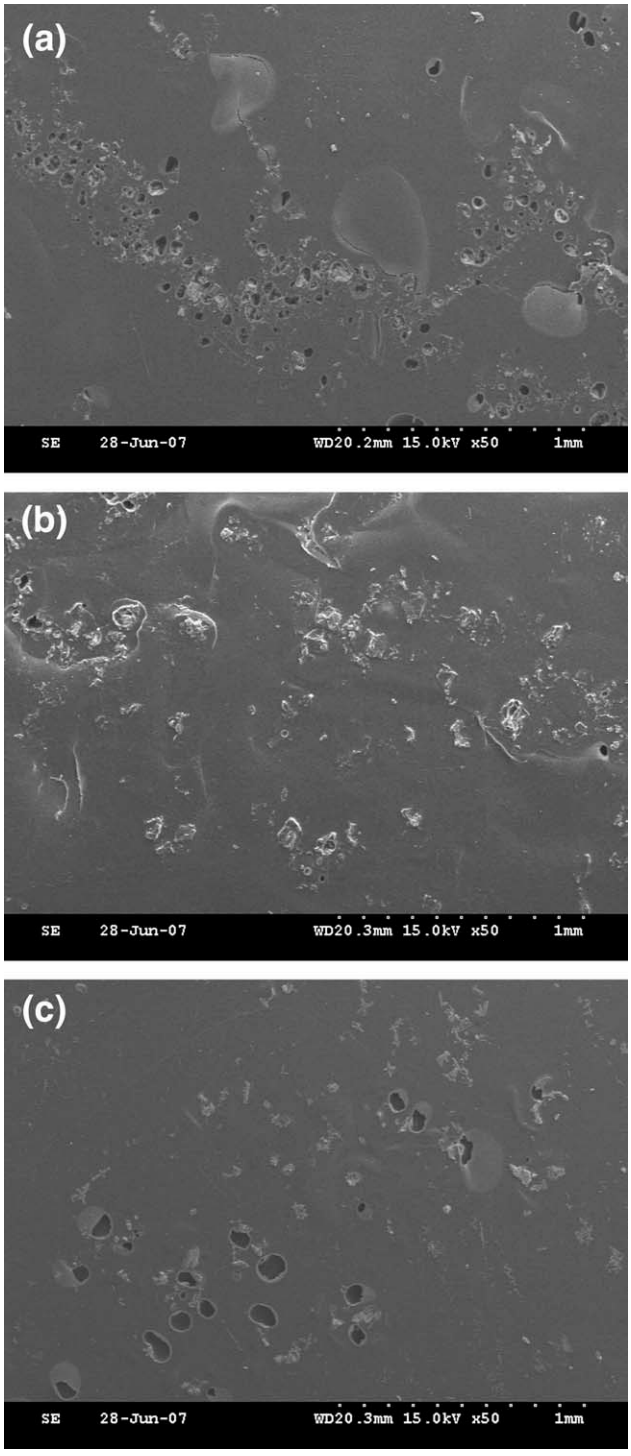

Figure 10 SEM images of the samples (a) PP_{15}-10, (b) O-PP_{15}-10, and (c) O-PP_{35}-10.

Compared with O-PP_{15}, the tensile strengths and elongation at breaking of the O-PP_{35} samples were lower. Even though, the same hydrophobic dispersant was used for series of samples, the tensile strengths and elongation at breaking were different. This difference highlights the effect of luminescent powder diameter. When the luminescent powder diameter was larger, the tensile strength and elongation at breaking of the material was lower.

CONCLUSIONS

The effect of different sizes and amounts of luminescent powder and hydrophobic dispersant on PP were discussed herein. MI, UV–Vis spectrophotometry, DSC, X-ray analysis, SEM, and mechanical tensile strength analysis have been used to analyze those samples. The MI of all samples decreased as the amount of luminescent powder was increased. Because of the rigidity of the luminescent powder, frictional stress between the materials was higher. O-PP_{15} samples had the higher MI than PP_{15} samples. This was due to plasticization of PP by the long alkane chains of the hydrophobic dispersant. The initial luminescence of the luminescent powder was 1151 mcd/m^2, whereas the initial luminescences of the respective samples with luminescent powder incorporated into PP were in the range 39–439 mcd/m^2. The initial luminescence of a sample is influenced by the hydrophobic dispersant and the amount and size of the luminescent powder. The afterglow time of the luminescent powder was also measured. Except for the O-PP_{35} samples with high luminescent powder amount, the O-PP_{15} samples displayed the longest afterglow times. Through DSC and X-ray analysis, the α crystal structure was identified in all of the samples. In addition, the O-PP_{35} samples were also found to contain the β crystal structure. Thirty-five micrometer luminescent powder acts as a nucleating agent and promotes the formation of the β crystal structure. The solubility of the luminescent powder in PP is poor; hence, the observation of interfacial separation in SEM images. This interfacial separation of the components lowers the tensile strength of the materials.

TABLE V
Tensile Strengths and Elongation at Breaking of the Samples

Code	Tensile strength at breaking (MPa)	Elongation at breaking (MPa)
O-PP_{15}-1	38	19
O-PP_{15}-3	35	17
O-PP_{15}-5	33	16
O-PP_{15}-10	31	11
O-PP_{35}-1	36	17
O-PP_{35}-3	32	14
O-PP_{35}-5	31	12
O-PP_{35}-10	30	9
PP_{15}-1	30	10
PP_{15}-3	28	9
PP_{15}-5	27	7
PP_{15}-10	25	5

The tensile strength and elongation at breaking of pure PP sample is 41 MPa and 23%.

References

1. Matsuzawa, T.; Aoki, Y.; Takeuchi, N.; Murayama, Y. J Electrochem Soc 1996, 143, 2670.
2. Miyamoto, Y.; Kato, H.; Honna, Y.; Yamamoto, H.; Ohmi, K. J Electrochem Soc 2009, 156, J235.
3. Dorenbos, P. J Electrochem Soc 2005, 152, H107.
4. Burnell-Jones, P. US Pat. 6,207,077 (2001).
5. Matsuzawa, T.; Aoki, Y.; Takeuchi, M.; Murayama, Y. In Proceedings of the 188th Meeting of the Electrochem Soc, Japan, 1995; 160.
6. Murayama, Y. Sci Am Jap 1996, 26, 20.
7. Takahashi, H.; Tanable, S.; Hanada, T. J Ceram Soc Japan 1995, 104, 332.
8. Pallila, F. C.; Levine, A. K.; Tomkus, M. R. J Electrochem Soc 1968, 115, 642.
9. Abbruscato, V. J Electrochem Soc 1971, 118, 930.
10. Blasse, G. Philips Res Rep 1969, 24, 131.
11. Blasse, G. J Solid State Chem 1986, 62, 207.
12. Qingmei, S.; Jinfei, H.; Maojun, W. Faguang Xuebao 1991, 12, 144.
13. Matsuzawa, T.; Aoki, Y.; Takeuchi, N. Electron Chem Soc 1996, 143, 2670.
14. Lin, Y.; Zhang, Z.; Tang, Z. Mater Chem Phys 2001, 70, 156.
15. Holsa, J.; Junger, H.; Lastusaari, M. Alloy Compd 2001, 323, 326.
16. Yamatoto, H.; Matsuzawa, T. J Luminescence 1997, 72/74, 287.
17. Qiu, J.; Kawasaki, M.; Tanaka, K.; Shimizugawa, Y.; Hirao, K. J Phys Chem Solids 1998, 59, 1521.
18. Qiu, J.; Hirao, K. J Solid State Commun 1998, 106, 795.
19. Katsumata, T.; Nabae, T.; Sasajima, K.; Matsuzawa, T. J Growth 1998, 183, 361.
20. Wang, D.; Yin, Q.; Li, Y.; Wang, M. J Luminescence 2002, 97, 1.
21. Sakai, R.; Katsumata, T.; Komuro, S. J Luminescence 1999, 85, 149.
22. Aboulfaraj, M.; Ulrich, B.; Dahoun, A.; G'Sell, C. Polymer 1993, 34, 4817.
23. Natta, G.; Gorradini, P.; Cesari, M. Rend Acad Naz Lincei 1956, 21, 365.
24. Padden, F. J.; Keith, H. D. J Appl Phys 1959, 30, 1479.
25. Turner-Jones, A.; Aizelwood, J. M.; Beckett, D. R. Makromol Chem 1964, 75, 134.